

Forward and reverse high-pressure transitions in bulklike AlAs and GaAs epilayers

U. D. Venkateswaran,* L. J. Cui,[†] and B. A. Weinstein

Department of Physics, 239 Fronczak Hall, State University of New York at Buffalo, Buffalo, New York 14260

F. A. Chambers

Amoco Technology Co., P.O. Box 3011, Naperville, Illinois 60566

(Received 24 May 1991)

We report Raman studies of the transformations between the zinc-blende (α) and high-pressure (β) phases of bulk GaAs and AlAs epitaxial films under increasing and decreasing hydrostatic pressure using a 300-K diamond-anvil press. The forward α - β thresholds, as measured by the simultaneous onset of opacity and loss of Raman signal, are $P'_\alpha = 12.4 \pm 0.4$ GPa for AlAs and $P'_\beta = 17.3 \pm 0.4$ GPa for GaAs. On decompression from 20 GPa or less, reversal to the zinc-blende state occurs in both materials with a hysteresis of 6–8 GPa; otherwise, GaAs enters a metastable phase. After reversal, the returning optical-phonon peaks exhibit asymmetric broadening and negative frequency shifts. Analogy to ion-bombarded GaAs shows that postreversal material is comprised of zinc-blende microcrystallites with diameters ~ 65 Å and ~ 175 Å in GaAs and AlAs, respectively. Thermodynamic considerations based on the hysteresis and microcrystallite size suggest that the surface energy per unit area for a β nucleus in a pure α matrix is ~ 0.04 – 0.15 eV/Å², in rough agreement with previous microscopic calculations for a rocksalt–zinc-blende AlAs/GaAs heterointerface. We propose that the kinetic homointerface in the bulk nucleation transitions is similar to the static sixfold-fourfold heterointerface involved in the superlattice phase changes discussed in the second paper.

I. INTRODUCTION

The fundamental character of pressure (P)-induced phase transitions in covalent semiconductors has been recognized since their discovery some 30 years ago.^{1–3} These strongly first-order transitions result from the need for closer packing in order to stabilize the relatively open tetrahedral lattice (α phase) against hydrostatic compression. The properties of the resulting high-pressure structures (β phase) reflect the basic competition between covalent, metallic, and ionic bonding in semiconductors.^{4–6}

Considerable optical, electrical, and x-ray measurements have established the underlying features of these phase changes.^{7–9} In typical homogeneous bulk semiconductors, the lowest pressure transition involves a change from fourfold to sixfold nearest-neighbor coordination with a 15–20% volume decrease.^{3,9} Group-IV and weakly ionic III-V materials adopt the body-centered-tetragonal β -Sn structure; this phase generally exhibits metallic (actually semimetallic) transport properties, and can be superconducting.^{7,8,10,11} Prototypical for this category is the Sn transformation, which occurs on warming above 286.2 K without compression. With increasing ionicity above 0.3 in III-V and II-VI compounds,⁴ the lowest pressure transition tends toward the B1 (rocksalt) structure,^{3,8} or, for intermediate ionicity cases, to distorted versions of this structure.⁹ The latter may have either narrow-gap or semimetallic character. The β phase of GaAs belongs to this category and is known to be semimetallic.^{2,11–13} The α - β transformation generally proceeds via a nucleation mechanism which can exhibit sluggish kinetics, requiring anywhere from seconds to hours for completion at room temperature.^{6–8}

For many materials the α - β transition reverses when the pressure is reduced, but for others, e.g., Si, Ge,¹⁴ and GaAs,^{15,16} opaque metastable states can be retained at 1 bar and 300 K. When reversal occurs, there is often considerable threshold hysteresis,¹³ as expected from the sluggish nucleation mechanism.^{6,17} However, the conditions required for reversal or for formation of a metastable state, and the properties of pressure-cycled semiconductor phases have been studied much less extensively compared to the work on forward transitions.

Initial attempts to describe these transitions theoretically, and to predict their thresholds, were based either on theories of elastic instability,¹⁸ or, more successfully, on semiempirical correlations emerging from the dielectric theory of ionicity.^{4,5} Progress in density-functional methods¹⁹ has led to microscopic treatments that correctly select the high- P phase from among known possibilities.^{20,21} These treatments show that several candidate structures—e.g., β -Sn, B1 and distorted B1, NiAs, simple hexagonal—can be energetically quite close; they also predict the α - β transition pressures in reasonable agreement with experiment.²²

The original motivation for the experiments reported in this paper (designated Paper I) on bulk GaAs and bulk AlAs films was to provide a benchmark for our results on high-pressure transitions in GaAs/AlAs superlattices (SL's) discussed in Paper II to follow. However, it soon became clear that the phase changes in homogeneous bulk GaAs and AlAs exhibit many interesting features that are still not well understood, and therefore warrant separate discussion. These features emerge in the present Raman measurements because, unlike many earlier studies, we pay as much attention to the reverse $\beta \rightarrow \alpha$ transi-

tion as to its forward counterpart.¹³ Experimentally, these aspects relate to the occurrence of reversal, its threshold hysteresis, and the postreversal condition of bulk GaAs and AlAs. We shall see that the physics of these phenomena depends strongly on the nucleation process inherent to the α - β phase change in semiconductors. Particularly important is the surface-energy density for pressure-induced nucleation of a β nucleus within zincblende (ZB) material. In our work, an experimental estimate of this key quantity is obtained.

Additionally, atmospheric oxidation has inhibited Raman experiments on bulk AlAs. Hence, besides exploring the bulk transitions in this substance (observed previously by visual means only²³), the present study fulfills a need to document the phonon pressure response in bulk ZB AlAs compared to related bulk and SL systems. Also we report here results for the negative pressure shift of TA(X) in GaAs that conform more closely to material trends correlated with the α - β transitions.

There are many interconnections between the experimental findings in Papers I and II, and the results for bulk GaAs and AlAs will bear strongly on our analysis of SL phase transitions. We hope to make clear that a unifying characteristic is the role of internal α/β interfaces—momentary *homointerfaces* in pure bulk solids, and static *heterointerfaces* in the SL's. In particular, the possibility is discussed that a fourfold-sixfold geometry proposed on theoretical grounds by Martin²⁴ exists at the surface of a β nucleus growing in an otherwise pure α matrix.

The present paper is organized into five sections. The comprehensive account of experimental procedures (Sec. II) that follows this introduction is intended to cover aspects common to both papers I and II. The Raman results for bulk GaAs and AlAs (Sec. III) are then described in four subsections dealing with (Sec. III A) phonon pressure response, (Sec. III B) forward and reverse α - β transformations, (Sec. III C) transition-induced microcrystallinity, and (Sec. III D) evidence for metastable

GaAs. The subsequent discussion of these results (Sec. IV) makes a connection to the energy density of internal α/β interfaces. We also consider briefly a correlation between TA(X) softening and the bulk α - β thresholds. Finally, the main conclusions in Paper I are summarized in Sec. V.

II. EXPERIMENT

The growth architectures of the bulklike AlAs and GaAs films studied in this work, designated BL1 and BL2, respectively, are listed in Table I. (Similar designations, SL1–SL6, are used to label the GaAs/AlAs superlattices discussed in Paper II.) The present samples are grown by molecular-beam epitaxy (MBE) without intentional doping on [001]-oriented semi-insulating *n*-type GaAs substrates. The desired film thicknesses are achieved according to the calibrated deposition rates of the growth apparatus, which have been determined by established x-ray and electron microscope analysis.²⁵ Since the films (2 μm of AlAs in BL1 and 8 μm of GaAs in BL2) contain several thousand monolayers, both may be considered bulklike for the purposes of these experiments. BL1 has a 1000-Å-thick GaAs cap layer to prevent atmospheric oxidation of the AlAs sandwiched underneath. Although this cap tends to attenuate the AlAs Raman signal for $P < 4.0$ GPa, viz., below the direct-to-indirect gap (Γ -X) crossover of GaAs,²⁶ it also provides a corroborative Raman calibration of the internal BL1 pressure (see below).

We employ a high-pressure diamond-anvil cell (DAC) to generate ruby-calibrated pressures up to 30 GPa at room temperature. This DAC is a standard National Institute of Science and Technology type²⁷ utilizing 0.35 carat type-I diamonds in a gasketed (Inconel X750, 250 μm initial thickness) opposed Bridgman-anvil configuration. The pressure chamber consists of a 200- μm -diam gasket hole between the diamond anvils filled with a 4 to 1 (by volume) methanol to ethanol medium;

TABLE I. Summary of sample characteristics and detected phase-transition pressures in GPa. P'_a and P'_g denote the forward α - β thresholds in AlAs and GaAs, respectively, and R' is the pressure where transparency returns on decompression from the P_{max} listed in brackets. Previous experimental and theoretical results are tabulated. The equilibrium thresholds fall roughly midway between the P' and R' . (See Sec. IV A, and Ref. 13.) S_{sub} denotes the (001) GaAs substrate.

Samples	BL1	BL2	Previous results		
Architecture	GaAs/AlAs/ S_{sub}	GaAs/ S_{sub}			
Thickness (μm)	0.1/2.0/ S_{sub}	8.0/ S_{sub}			
P'_a	12.4 \pm 0.4		12.3 \pm 0.4 ^a	9.0 ^b	7.6 ^c
P'_g	17.2 \pm 0.4	17.3 \pm 0.4 ^d	17.2 \pm 0.4 ^a	17.0 \pm 0.5 ^e	16.0 \pm 1.6 ^f
			17.2 \pm 0.7 ^g	17.0 ^b	16.0 ^e
R'	6.0 \pm 1.5	9.0 \pm 1.5			
[P_{max}]	[\sim 14 GPa]	[\sim 18 GPa]			

^aReference 23.

^bReference 24, theory.

^cReference 22, theory.

^dCap layer.

^eReference 9.

^fReference 11.

^gReference 12.

this mixture remains hydrostatic at 300 K until 9.5 GPa, above which it develops pressure gradients. These gradients, which at 20 GPa can be as large as 3–4 GPa across the gasket hole, are minimized by annealing the DAC at $\sim 70^\circ\text{C}$ – 75°C for about an hour. After annealing, the observed pressure variation across the gasket hole is no greater than 1 GPa at 20 GPa, and less at lower pressures.

Sample preparation for the DAC is usually not routine because of the small dimensions required to reach high pressure. Specimens of BL1 and BL2 are thinned on the substrate side to a total thickness of 15–25 μm , which gives sufficient transparency above 4 GPa to permit visual observation of their phase transitions.²⁶ To accomplish the thinning without producing numerous dislocations in the epitaxial films, the GaAs substrates are lapped mechanically to $\sim 80 \mu\text{m}$, and then polished chemically with 5% NaOCl solution on a soft semiconductor-grade polishing pad until reaching the final thickness.²⁸ It is important to protect the epitaxial-layer side and sample edges with sufficient mounting wax. After cleaning with acetone and distilled water, the samples are gently cleaved into $\sim 50 \mu\text{m} \times 70 \mu\text{m}$ rectangular platelets bordered by $\{110\}$ cleavage planes normal to the film surface. These specimens are then loaded into the DAC sample chamber by means of a sharp dissecting needle.

Besides the sample, several tiny ruby chips usually are loaded into the gasket hole to calibrate the pressure by the *R*-line fluorescence technique.²⁷ Use of multiple ruby chips allows correction for nonhydrostatic gradients that persist after annealing. The pressure at a given specimen site is determined by linearly interpolating the *R*-line frequencies recorded at various locations in the gasket hole to that specimen site. Above 9.5 GPa, this procedure enhances the precision of measuring the specimen's *internal* pressure. The precision can be gauged by comparing the interpolated ruby results with pressures predicted by Raman measurements of the GaAs LO(Γ) phonon frequency at the same specimen sites. (The signal is from the cap layer in BL1.) For this purpose we use the calibration in Fig. 1, obtained by fitting *all* pretransition Raman data on the bulk GaAs film BL2. The agreement between the ruby and Raman site pressures is generally ± 0.4 GPa. This agreement is sufficiently consistent that the GaAs LO(Γ) peak could be used to determine the pressure when ruby was omitted from one loading of sample BL1 intended for x-ray studies.²⁹

Particular care is taken not to “overshoot” the phase-transition thresholds. As an expected threshold is approached, the pressure is increased in steps of ≤ 0.5 GPa followed by long periods (~ 1 h) of annealing. Ruby and Raman measurements are recorded before and after each increase and annealing period, and the sample's visual appearance is examined and stored on videotape. We detect the onset of a transition by the nucleation of opaque β domains showing no ZB Raman peaks. These domains grow and coalesce within the transparent ZB α phase until the entire specimen is converted. (See the photographs in Ref. 23 and Paper II for examples of this process.) In some runs the transition goes immediately to completion, while, in others, nonhydrostatic conditions preserve the

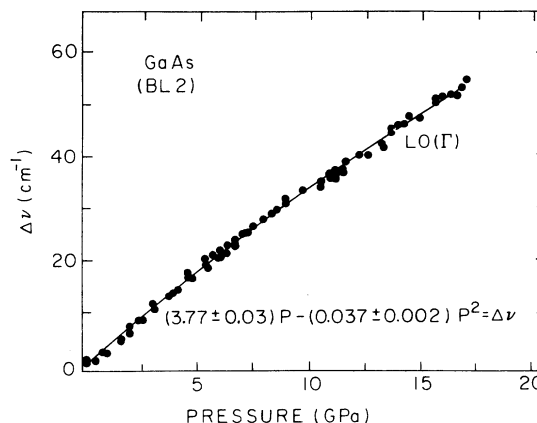


FIG. 1. Measured pressure shift of the GaAs LO(Γ) frequency in the 8- μm -thick MBE film of sample BL2. Solid curve and displayed equation give the quadratic best fit to ~ 70 data points. This was used to corroborate DAC pressures measured in the present work by the ruby interpolation technique. (See text.)

specimen in a partially transformed state until the pressure is raised further. We take the transition threshold to be either the site pressure at the transparent-opaque boundary, or that recorded immediately after darkening at the center of a fully transformed specimen; the quoted pressure is always the interpolated ruby value, except for a single BL1 run calibrated directly by the GaAs LO(Γ) peak. Since repeated measurements in independent DAC loadings of each sample (2 for BL1, 3 for BL2, and also 2 each for the SL's in Paper II) *agree with each other* within the ± 0.4 GPa site precision, we believe that this margin is a fair assessment of the overall uncertainty in the forward (increasing pressure) α - β thresholds. The anticipated uncertainty in the β - α reverse thresholds is probably ± 1.5 GPa, due to the larger steps employed during pressure reduction.

The Raman measurements are performed at 300 K using a standard double monochromator with 1800 groove/mm holographic gratings in combination with either photomultiplier, or intensified Si-diode-array detectors, and computer-controlled data acquisition and processing. We incorporate custom-built microprobe fore optics to focus the Kr^+ or Ar^+ laser excitation into the DAC, and collect the backscattered light. The microprobe achieves $250\times$ magnification, with a 50 mm working distance, and $1/f = 1.4$ collection efficiency.³⁰ Video recording of pressurized specimens using a color television camera mounted on an optical port is part of our standard operation. With this system, Raman scattering can easily be measured from ~ 10 - μm -diam isolated spots within the DAC—the resolution being confirmed by placing pinholes of appropriate size at a secondary focus within the microprobe. This ability is important for probing as close to a phase boundary as possible. Incident laser powers of ≤ 30 mW focused to 10 μm at the specimen are used; this is at least a factor of 2 below the observed levels for damage at low pressures where absorption is greatest. Both the present work and

that discussed in Paper II employ the same Raman-scattering apparatus.

III. RESULTS

A. Phonon pressure response in the ZB phase

Typical ZB-phase Raman spectra recorded for AlAs and GaAs at 1 bar and 8.5 GPa are shown in Fig. 2. The spectra are a composite of data from both samples. The traces include the one-phonon zone-center longitudinal optic [LO(Γ)] and transverse optic [TO(Γ)] peaks of AlAs and GaAs, and the two-phonon acoustic-overtone [2TA] band of GaAs; the latter exhibits structure similar to other tetrahedral semiconductors due to zone-boundary critical points.³¹ These are the most intense Raman features observed. We find no sign of the AlAs 2TA band, and, in particular, of the 2TA(X) peak which is expected in AlAs at $\sim 220 \text{ cm}^{-1}$ (1 atm) by simple frequency scaling relative to GaAs. This absence is probably due to the GaAs-cap layer in sample BL1—the AlAs 2TA band being dominated by cap-layer scattering [e.g., by the GaAs 2A(K) feature] because of greater resonance enhancement in GaAs than AlAs with the available laser lines. Although the cap-layer component of the BL1 spectra ($\nu < 330 \text{ cm}^{-1}$) has not been included in Fig. 2, we find that it does not differ significantly at any pressure from the pure GaAs BL2 results.³²

At 1 bar the GaAs and AlAs one-phonon peaks exhibit the standard tetrahedral selection rules for unpolarized backscattering at a (001) surface—namely, LO(Γ) is al-

lowed and TO(Γ) is dipole forbidden.³³ With increasing pressure, the GaAs LO(Γ) peak strengthens according to the expected pressure-tuned resonance behavior found in earlier work.³⁴ In addition, “forbidden” TO(Γ) scattering appears with increasing intensity in both the AlAs and GaAs spectra until it becomes comparable to LO(Γ). This occurs in the present bulk films and the SL’s treated in Paper II, and it also was observed in previous DAC work on bulk GaAs.³⁴ Our studies on substrate-backed and free-standing specimens indicate that the TO(Γ) enhancement arises from allowed forward scattering of reflected laser light from the specimens’ back surface,³⁵ which only becomes optically accessible at elevated pressures.^{26,36}

The pressure dependence of the AlAs and GaAs phonon frequencies observed in samples BL1 and BL2 is plotted in Fig. 3. Following standard trends, the optic frequencies increase and the zone-boundary transverse-acoustic phonons soften under compression.³⁷ The solid curves are least-square fits to the data, and the corresponding best-fit parameters and linear mode Grüneisen constants, $\gamma = -d(\ln \nu)/d(\ln V)$, are listed in Table II. Variations between the γ ’s found in this work and the literature values included in Table II can be attributed to the different compression methods (uniaxial versus hydrostatic) and/or pressure ranges of the data sets. We note that the LO(Γ) and TO(Γ) Grüneisen constants for AlAs are similar to each other and to those of GaAs, as expected. Although there are no previous reports of the optical-phonon pressure shifts in bulk AlAs, Table II shows that the present results are similar to typical

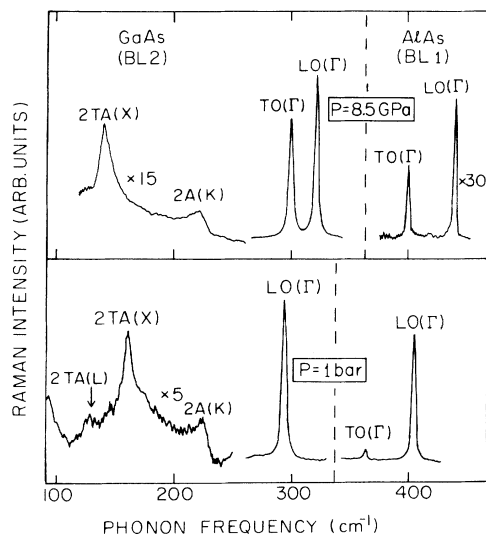


FIG. 2. Room-temperature Raman spectra for ZB-AlAs in sample BL1 (right of dashed line) and ZB-GaAs in sample BL2 (left of dashed line) at 1 bar and 8.5 GPa under 647.1 nm excitation. For sample BL1, scattering from the GaAs cap layer is not shown. Data at 1 bar were recorded outside the DAC, and that at 8.5 GPa with both samples loaded side-by-side in the DAC. Labels identify first-order optical-phonon lines of AlAs and GaAs, and major critical point features in the acoustic-overtone band of GaAs.

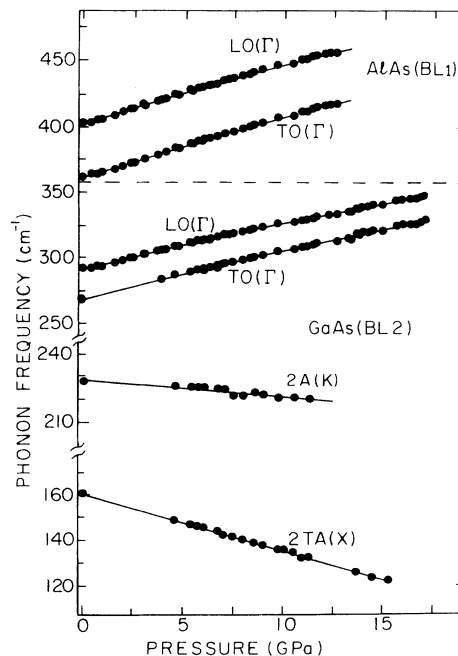


FIG. 3. Phonon frequencies as a function of hydrostatic pressure for the prominent AlAs and GaAs Raman features measured for samples BL1 and BL2. Solid curves are least-square fits (parameters in Table II) to the data points.

TABLE II. Quadratic-fit parameters ($\nu = \nu_0 + aP + bP^2$) for the pressure shifts of the AIA's (BL1) and GaAs (BL2) phonon frequencies plotted in Fig. 3, and corresponding linear Grüneisen constants γ . Bulk moduli used to calculate γ are from Ref. 38; the overall uncertainties in the present γ 's are $\pm 5\%$ for LO(Γ) and TO(Γ), $\pm 8\%$ for 2TA(X), and $\pm 10\%$ for 2A(K). Previous results are given for comparison.

Sample	Phonon mode	$\nu(0)$ (cm^{-1})	a $\left[\frac{\text{cm}^{-1}}{\text{GPa}}\right]$	b $\left[\frac{\text{cm}^{-1}}{\text{GPa}^2}\right]$	Grüneisen constant γ		
					Present work	Previous expts.	
GaAs	LO(Γ)	291.2	3.76	-0.035	0.97	1.23 ^a 1.09 ^c 1.29 ^c	0.93 ^b 0.81 ^d 1.05 ^d
	TO(Γ)	268.1	3.95	-0.032	1.11		
	2A(K)	228.0	-0.72	0	-0.24	-0.4 ^a	0.04 ^c
	2TA(X)	160.3	-2.5	0	-1.20	-1.62 ^a	-1.92 ^c
AIA's	LO(Γ)	402.1	4.81	-0.049	0.93	0.86 ^{b,f}	1.06 ^g
	TO(Γ)	360.8	4.86	-0.038	1.05	0.99 ^{b,f}	

^aTrommer, Müller, and Cardona (1980), Ref. 34.

^bReference 39.

^cWickboldt *et al.*, Ref. 40; Raman studies with $\lambda_l = 1.06 \mu\text{m}$ averaged for [001] and [111] uniaxial stress.

^dHünemann *et al.*, Ref. 40; reststrahlen studies averaged for [001] and [111] uniaxial stress.

^eYu and Welber, Ref. 34.

^fConfined AIA's-like mode in a 55 Å/44 Å GaAs/AIA's SL.

^gReference 41; confined AIA's-like mode in a 20 Å/60 Å GaAs/AIA's SL.

findings for AIA's confined modes in SL's.^{39,41} The softening of the GaAs TA(X) mode is discussed in Sec. IV B in relation to the α - β transition threshold.

B. Forward and reverse α - β transformations

As noted above, visual microscopy provides a convenient means for detecting the appearance of the opaque β phase. In addition, visual studies can yield substantial information about the transition kinetics. For the bulk GaAs film BL2, we find that the α - β change is rather sluggish, with the opaque domains expanding by roughly a few μm per minute. This is similar to the α - β kinetics in many other bulk semiconductors, e.g., Si, GaP, InSb, etc.⁶⁻⁸ In contrast, the AIA's transition in sample BL1 exhibits comparatively rapid kinetics, going to completion after (at most) a few tenths of a second, during which momentary opaque-transparent boundaries, with well-defined but undetermined crystallographic orientations, can appear. There is no ambiguity in visually identifying the AIA's transition in sample BL1, since this occurs some 5 GPa below the analogous α - β change in the sample's GaAs substrate and cap layer. The latter transformation, however, must be detected by Raman scattering.

Pressure-Raman data illustrating the α - β transitions of bulk AIA's and bulk GaAs in samples BL1 and BL2 are presented in Figs. 4(a) and 4(b), respectively. The rectangular inset-sketches depict the specimen morphology and the laser focus position at the indicated pressures.

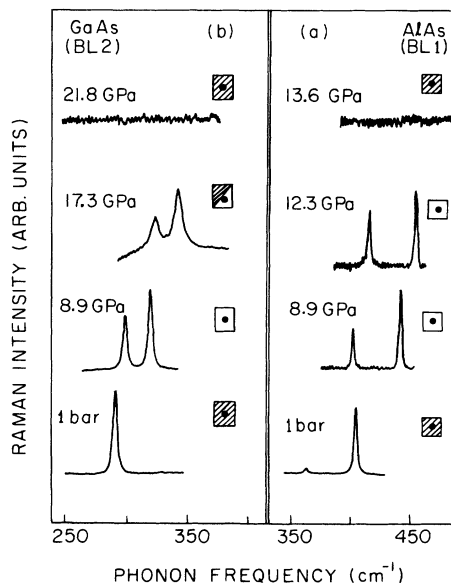


FIG. 4. Zinc-blende-phase LO(Γ) and TO(Γ) Raman peaks ($\lambda_l = 647.1 \text{ nm}$) of AIA's (a), and GaAs (b) at various increasing pressures through their α - β phase transitions at $P_g^t = 12.4 \pm 0.4 \text{ GPa}$ and $P_g^t = 17.3 \pm 0.4 \text{ GPa}$, respectively. After the transitions only a flat background can be detected. Visual specimen appearance (i.e., opaque or transparent) and laser location are indicated by the shading and solid circle in the rectangles.

The upper two panels of each figure show that the ZB LO(Γ) and TO(Γ) peaks of AlAs and GaAs disappear coincident with the onset of opacity in the respective samples. No β -phase Raman signal could be detected at high pressure in samples BL1 and BL2.

Unannealed pressure gradients enable us to catch sample BL2 in a state of incomplete transition with its ZB-phase LO(Γ) and TO(Γ) peaks persisting in the transparent region of the specimen. This is shown in the 17.3-GPa data of Fig. 4(b). The presence of these gradients is also indicated by the broadening of the GaAs peaks at 17.3 GPa compared to the Fig. 4(b) data at 8.9 GPa and 1 atm. In contrast, for sample BL1 the AlAs optical-phonon peaks at 12.3 GPa [Fig. 4(a)] are not broadened with respect to the $P < 9.5$ GPa hydrostatic results. This shows that more complete annealing occurs at 12.3 GPa than at the higher α - β threshold of GaAs, and this, combined with the faster kinetics of the AlAs transition, explains why sample BL1 could not be retained in a mixed α - β state. Using the pressure-calibration procedures described in Sec. II, we find in samples BL1 and BL2 that the α - β forward thresholds are $P_a^f = 12.4 \pm 0.4$ GPa for bulk AlAs, and $P_g^f = 17.3 \pm 0.4$ GPa for bulk GaAs. The present values agree well with the earlier visual observation for AlAs,²³ and with the accepted x-ray determinations for GaAs (Refs. 9 and 12) corresponding to organization of the orthorhombic GaAs-II lattice.¹³ These results are included for comparison in Table I along with some theoretical predictions.

Just as the onset of opacity signals transformation to a semimetallic or narrow-band-gap phase, the return of visual transparency on decompression is clear evidence for a down-cycle transition to a semiconducting state with band gap exceeding 1.65 eV. We find, in the bulk films BL1 and BL2 (and in the SL's studied in Paper II), that this may or may not occur depending on the maximum pressure P_{\max} reached during the preceding up cycle. The critical maximum seems to be ~ 20 GPa. If P_{\max} is below this value, transparency is regained. However, if P_{\max} exceeds 20 GPa, all GaAs-containing samples return to 1 atm with their GaAs components in a metastable phase that remains opaque during the entire down cycle.¹⁵ This will be discussed further in Sec. III D below.

In those runs where transparency does return, we observe threshold hysteresis compared to the previous up-cycle transitions; this hysteresis is ~ 6 GPa for AlAs and ~ 8 GPa for GaAs. Similar hysteresis is well known for the forward and reverse α - β transitions in other bulk semiconductors.⁶⁻⁸ It can be related (see Sec. IV) to the surface formation energy of a β nucleus within an α matrix. The observed pressures R^f at which BL1 and BL2 regain visual transparency are listed with the associated P_{\max} in Table I.

The return of a transparent state does not guarantee reversal to the ZB phase. However, the AlAs and GaAs Raman spectra in Fig. 5 demonstrate that the latter is, indeed, the case for samples BL1 and BL2. The Fig. 5 panels compare (from bottom to top) pretransition data with spectra recorded after the samples again become transparent during cycles in which $P_{\max} < 20$ GPa. For

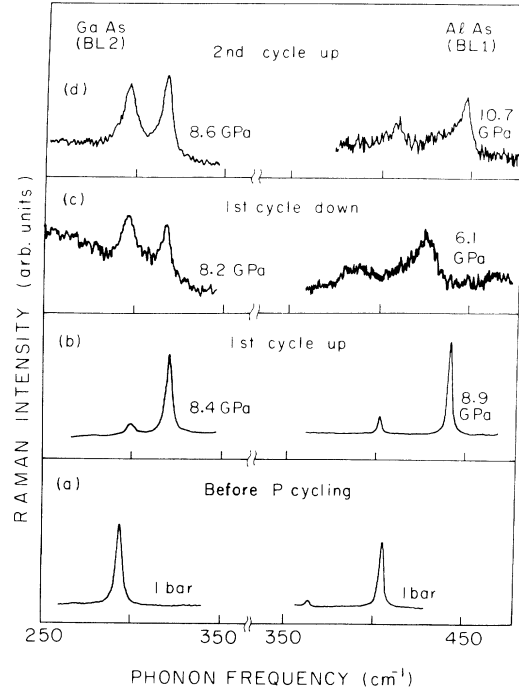


FIG. 5. Pressure-cycling study of the TO(Γ) and LO(Γ) Raman peaks ($\lambda_i = 568.2$ nm) in AlAs and GaAs before transforming, and after reversal to the ZB phase. (a) Pristine BL1 and BL2 samples outside the DAC. (b) Pretransition spectra taken on compression. (c) Postreversal spectra on decompression from above P_a^f for BL1 and P_g^f for BL2 ($P_{\max} < 20$ GPa). (d) Postreversal spectra of the same specimens on recompression from near 1 bar. Note in (c) and (d) that the ZB peaks have reappeared, but show low-energy broadening and violation of the TO(Γ) selection rule compared to similar pressure spectra in (b).

both AlAs and GaAs, the ZB LO(Γ) and TO(Γ) peaks reappear in consonance with transparency during decompression. The peaks are weaker and broader than before, but they grow in strength and sharpen as the pressure is reduced to near 1 bar and then raised to 8–11 GPa. (See top two figure panels.) Such changes show that the reverse β - α transitions are extremely sluggish in these bulk samples, with the initial fraction of returning ZB material increasing during the ~ 20 h of each experiment. It is difficult to assess the extent that reversal approaches completion, since samples often acquire a hazy appearance indicating that internal light scattering from transition-induced microcrystalline domains (see below) affects transmission. However, in order to regain visual transparency, we believe the reversal fractions probably exceed 90%—assuming a typical direct absorption of $\sim 5 \times 10^4$ cm⁻¹ for any opaque β material remaining within the 2 μm of AlAs and 15 μm of GaAs in samples BL1 and BL2, respectively.^{13,26}

C. Transition-induced microcrystallinity

Evidence for transition-induced ZB microcrystals appears in the increased disorder suggested by the asymmetric peak broadening, and breakdown of the TO(Γ)

selection rule after reversal [compare Figs. 5(b)–5(d)]. Additionally, there is a residual negative frequency shift of the LO(Γ) [and to a lesser extent the TO(Γ)] peak in postreversal material, from which size estimates of the microcrystalline domains can be made.¹⁵ Let us consider these effects more quantitatively.

Whenever possible, specimens were retrieved from the DAC to investigate their 1 bar phases after pressure cycling, and typical Raman results for GaAs in sample BL2 are displayed in the middle two panels of Fig. 6. Comparing Figs. 6(a) and 6(b) we find the following: after reversal the ZB LO(Γ) peak falls $3.0 \pm 0.5 \text{ cm}^{-1}$ below the original 1 bar LO(Γ) frequency, the ZB TO(Γ) and LO(Γ) peaks in cycled samples exhibit at least a factor of 2 asymmetric broadening toward low energy, and the postreversal TO(Γ) intensity is comparable to that of LO(Γ) (whereas previously it was not detected). Similar Raman spectral changes have been studied extensively for the damaged surface region of GaAs subjected to variable-dosage ion bombardment.^{42,43} In that situation, the mag-

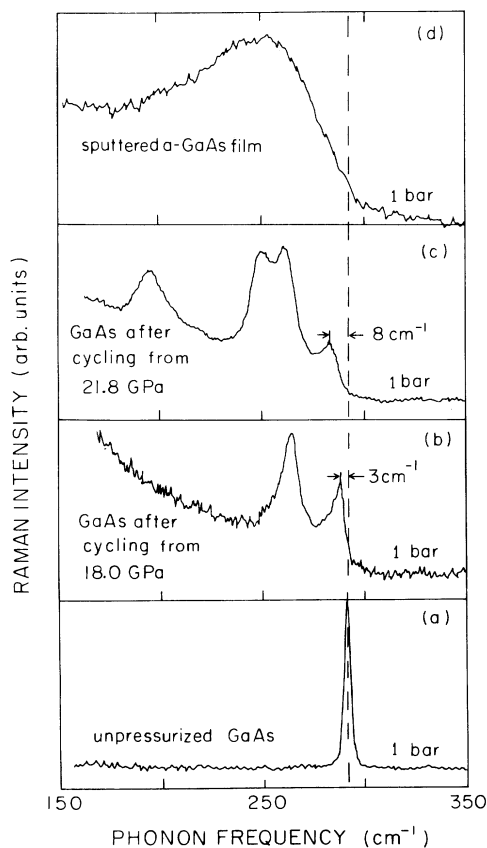


FIG. 6. Comparison of 1 bar GaAs Raman spectra in (a) the pristine BL2 film showing the LO(Γ) peak marked by the dashed line; (b) a BL2 specimen after transformation and reversal showing a 3 cm^{-1} redshift of LO(Γ); (c) the characteristic four-peak spectrum of metastable GaAs (again in BL2); and (d) an as-grown sputtered amorphous GaAs film [reproduced from Zallen *et al.* (Ref. 43)]. Note that the 8 cm^{-1} difference between the highest peak frequency in (c) and LO(Γ) cannot be explained by ZB microcrystallites.

nitude of the induced redshift and the asymmetric broadening of the LO(Γ) peak were explained by a spatial-correlation model⁴⁴ with finite-size spherical regions representing microcrystalline domains of ZB GaAs. Based on direct application of this model, our LO(Γ) results indicate that the GaAs specimens undergoing β - α reversal return to 1 bar containing a mosaic of ZB micrograins having $\sim 65 \text{ \AA}$ average diameter. Given such small domains, it is not surprising to have sufficient orientational disorder to relax the TO(Γ) selection rule.

A similar analysis for AlAs in retrieved BL1 samples is hampered by attenuation losses due to the sample's GaAs cap. However, comparisons between ZB spectra recording during the first- and second-cycle compressions at corresponding pressures in the range 6–8 GPa (where the cap layer is transparent) show a postreversal shift in the AlAs LO(Γ) peak of $-0.8 \pm 0.5 \text{ cm}^{-1}$. This suggests a larger micrograin diameter in reversed AlAs, which would be $\sim 175 \text{ \AA}$ based on the Ref. 42 results. Hence it appears from these estimates that the transition-reversal process produces a much finer microcrystalline mosaic in GaAs than in AlAs.

D. Evidence for a metastable phase of GaAs

A detailed Raman study of the metastable GaAs phase retained in samples BL1 and BL2 has been reported elsewhere by the authors.¹⁵ Here we summarize the main points of that work in relation to the α - β transition and its reversal.

Figure 6(c) shows the Raman spectrum of sample BL2 after cycling to 1 bar from $P_{\text{max}} = 21.8 \text{ GPa}$. Note that the highest frequency peak is shifted by -8 cm^{-1} from the original 1 bar LO(Γ) position. For ion-bombarded GaAs, the LO(Γ) Raman peak exhibits a similar shift to lower frequency with increasing fluence. In this case, the maximum observed shift of the ZB LO(Γ) peak is -4.5 cm^{-1} , corresponding to a correlation diameter of $\sim 45 \text{ \AA}$.⁴² Within the spatial-correlation picture, the domain size required to cause the shift of -8 cm^{-1} found in sample BL2 after pressure cycling [Fig. 6(c)] would be $\sim 6 \text{ \AA}$. This is far below any stable microcrystalline diameters observed in the ion-implantation work. For heavier implantation doses, the Raman scattering becomes dominated by a growing broadband component resembling the spectrum of amorphous (α -) GaAs.⁴³ In contrast, the four peaks in Fig. 6(c) are much too sharp to have an amorphous origin, as is apparent by comparison to the Fig. 6(d) trace for sputtered α -GaAs.⁴³

Figure 7 shows that similar results are found for other GaAs-containing samples which do not regain transparency on decompression. Panels 7(a)–7(d) represent, respectively, spectra for melt-grown GaAs, a 1000 \AA GaAs film (i.e., the BL1 cap layer), a free-standing GaAs/AlAs SL, and the 8 \mu m GaAs film in BL2—each retrieved from the DAC after pressurization above 20 GPa. The four traces exhibit similar peaks that are sharp compared to the α -GaAs spectrum shown in Fig. 6(d), and they have their highest peak frequency some 8–10 cm^{-1} below the original ZB LO(Γ) position. Furthermore, preliminary 1 bar x-ray studies of sample BL1 after

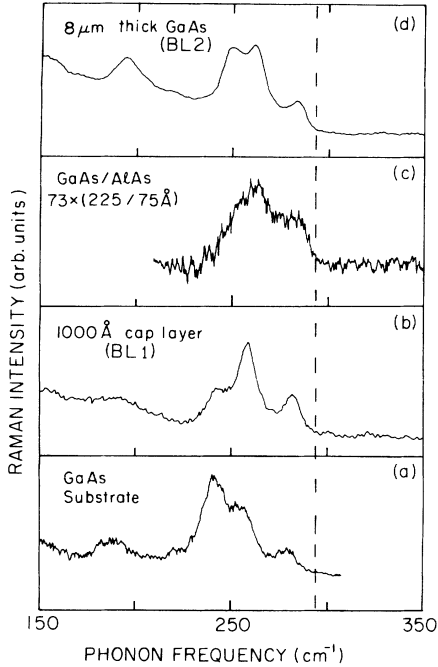


FIG. 7. Raman spectra at 1 bar after reaching $P_{\max} > 20$ GPa for (a) GaAs substrate material, (b) the epitaxial face of sample BL1, (c) SL2 studied in paper II, and (d) the bulklike GaAs overlayer in sample BL2. Dashed line marks the ZB LO(Γ) position. The metastable GaAs signature is evident even for the AlAs-containing samples shown in (b) and (c).

equivalent pressure cycling do not show the halo Laue patterns characteristic of amorphous solids, although the actual crystal structure was not identified.²⁹ (Also see Ref. 13.) Consequently, the 1 bar Raman spectra of Fig. 7 have been assigned to a metastable microcrystalline GaAs phase, different from its ZB and amorphous states; the most likely candidate structures are sixfold coordinated intermediates between the known high-pressure forms, GaAs II (distorted rocksalt) and GaAs III (distorted hexagonal).^{12,16}

Finally, we find that all retrieved samples not regaining transparency (BL and SL alike) show no AlAs Raman signal. Since this may simply reflect weak intensity, we are unable to determine whether or not a metastable AlAs phase occurs.

IV. DISCUSSION

A. Energy density of the internal α/β homointerface

It is well known for first-order phase transitions proceeding via a nucleation mechanism that the surface energy required to grow nuclei of β material within an α matrix gives rise to a kinetic barrier against β nuclei smaller than a certain critical size.¹⁷ This barrier also leads to the hysteresis between forward and reverse thresholds commonly observed in such phase transitions. It is of interest here (also for the discussion in Paper II) to estimate the α/β surface energy based on our observa-

tions of hysteresis and microcrystallite size for the GaAs and AlAs transitions.

We must consider, as a function of pressure, the difference in Gibbs free energy between a pure α phase and an α phase containing a β nucleus of radius r .⁶ This has both volume and surface terms, and for a spherical embryo at temperature T and pressure P , it can be expressed as

$$\Delta G^{\beta\alpha} = \frac{4}{3}\pi r^3 \left[\Delta u^{\beta\alpha} - T\Delta s^{\beta\alpha} + P \left(\frac{\Delta V}{V} \right)^{\beta\alpha} \right] + E^{\beta\alpha} + 4\pi r^2 \sigma_0^{\beta\alpha}. \quad (1)$$

Here $\Delta u^{\beta\alpha}$ and $\Delta s^{\beta\alpha}$ are the changes in energy density and entropy density on going from α to β , $(\Delta V/V)^{\beta\alpha}$ is the fractional transition volume change, $E^{\beta\alpha}$ accounts for the strain induced by the α matrix within the volume of the β nucleus, and $\sigma_0^{\beta\alpha}$ is the energy per unit area of the α/β homointerface (always positive and the same, whether we consider β in α , or vice versa). For fluctuations to favor growth, $\Delta G^{\beta\alpha}$ must decrease as r increases incrementally. This only occurs for radii exceeding a critical value r^* at which Eq. (1) is a maximum. The hysteresis is introduced by recalling that the bracketed expression in Eq. (1) vanishes at P_0 , the equilibrium pressure for transition between the two phases considered in isolation. (P_0 cannot be measured precisely because of the hysteresis. See Ref. 13.) Expanding the bracket to first order in $(P - P_0)$, neglecting $E^{\beta\alpha}$ since there is likely to be numerous strain-relieving dislocations at the growth interface, and performing the maximization yields⁶

$$r^* \simeq - \frac{2\sigma_0^{\beta\alpha}}{(P - P_0) \left(\frac{\Delta V}{V} \right)^{\beta\alpha}} \quad (2)$$

for the critical radius, and

$$\Delta G^{\beta\alpha}(r^*) = \frac{4}{3}\pi r^{*2} \sigma_0^{\beta\alpha} \quad (3)$$

for the barrier height. Note that because $(\Delta V/V)^{\beta\alpha} < 0$, both r^* and the barrier height decrease with increasing pressure above P_0 until fluctuations overcome the barrier, and growth proceeds for $r > r^*$ at the observed threshold $P = P^t$. Analogous equations apply for the β to α reverse transition, with the obvious exchange of superscripts, and the realization that the volume change is now positive so that reversal can occur only at $P = R^t < P_0$. Since $\sigma_0^{\beta\alpha}$ is the same for the forward and reverse transitions in this simple model, we expect that r^* will correspond to $(P - P_0) = (P^t - R^t)/2$, which provides the desired link to the observed hysteresis.

If one now considers what minimum sizes of β nuclei might be likely, we find that the possible range of r^* is restricted by experiment. The redshifts of LO(Γ) observed in postreversal spectra imply that nuclei exist with radii ~ 35 Å in GaAs and ~ 90 Å in AlAs. On the other hand, the GaAs ion-implantation studies find no regions of microcrystalline correlation with stable radii less than ~ 20 Å before increasing dosage produces amorphization.^{42,43} Using these limits, the typical value

$(\Delta V/V)^{\beta\alpha} = -18\%$,^{12,22} and the measured hysteresis (from Table I), we estimate from Eq. (2) that the areal energy density for the α/β homointerface is in the range $\sigma_0^{\beta\alpha} = 0.05 - 0.08 \text{ eV}/\text{\AA}^2$ for GaAs, and $\sigma_0^{\beta\alpha} = 0.04 - 0.15 \text{ eV}/\text{\AA}^2$ for AlAs.

These estimates are of some interest, both for the present treatment of α/β homointerfaces in bulk GaAs and AlAs, and for the energy of α/β heterointerfaces between the layers of GaAs/AlAs SL's considered in Paper II. Martin²⁴ has calculated the total energies of GaAs/AlAs SL's in various mixed-coordination fourfold-sixfold geometries using microscopic local-density-functional methods.^{45,46} He finds that the energy of a fourfold-sixfold SL formed by joining ZB GaAs (fourfold) to NiAs-structure AlAs (sixfold) in the [111] stacking sequence As--GaAs-Al-As-- is 0.7 eV/atom-pair higher than the energy average (by mole fraction) of the separate constituents. This yields an interface energy density of $\sim 0.05 \text{ eV}/\text{\AA}^2$, which is in fair agreement with the Eq. (2) estimates. To put the numbers in perspective, the excess nucleation energy calculated by Martin corresponds to roughly 0.4 broken bonds of GaAs or AlAs (1.6 eV each for GaAs and 1.89 eV each for AlAs) (Ref. 47) per hexagonal unit-cell cross section in a (111) ZB plane.⁴⁸

An alternative macroscopic approach is to model the interface of a β nucleus within an α matrix by an array of dislocations such as are formed at a grain boundary.⁴⁹ The interface energy should then be given by an expression similar to the Read-Shockley formula,⁵⁰

$$\sigma_0 = \frac{1}{\lambda_0} \frac{\mu a_0^2}{4\pi(1-\nu)} (C - \ln\theta), \quad (4)$$

where λ_0 is the distance between dislocations, μ and ν are the shear modulus and Poisson's ratio, a_0 is the lattice constant (approximately equal to the Berger's displacement), θ is the grain-boundary angle, and C is the dislocation core contribution which we take to be 0.23 following Ref. 50. Evaluating Eq. (4) for the grain-boundary angle (27°) where the energy density achieves a broad maximum, one finds that Martin's fourfold-sixfold energy density (i.e., $0.05 \text{ eV}/\text{\AA}^2$) corresponds to the separation $\lambda_0 \approx 16 \text{ \AA}/\text{dislocation}$ for both GaAs and AlAs. This is about two-thirds of the r^* value obtained when the same energy density is used in Eq. (2). This seems reasonable considering the significant volume decrease and coordination change that occur during the α - β phase transition.

B. TA(X) softening and the α - β transition

An interesting, but as yet empirical, correlation has been proposed between the negative Grüneisen constant of the TA(X) mode and the measured α - β transition pressure in bulk tetrahedral semiconductors.^{51,37} This correlation is displayed in Fig. 8. Although surprisingly well followed for many different-ionicity materials, previous experiments have suggested that GaAs was an exception.³⁴ However, this is not confirmed by the present work; the GaAs $\gamma_{\text{TA}(X)} = -1.2 \pm 0.1$ obtained from a linear fit to our data (Fig. 3) falls reasonably within the Fig. 8 correlation. It is difficult to explain the discrepan-

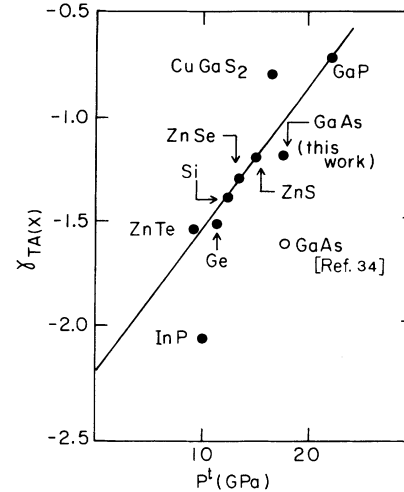


FIG. 8. Empirical correlation between the TA(X) Grüneisen constant and the α - β threshold pressure obeyed by many semiconductors. The present GaAs result satisfies the correlation much better than previous findings. (See text.)

cy with the earlier results.

Despite this success for GaAs, we view the proportionality between $\gamma_{\text{TA}(X)}$ and the observed P' with caution. Because of the large and material-dependent hysteresis associated with the α - β transition, it would be preferable to look for a correlation between $\gamma_{\text{TA}(X)}$ and the true equilibrium threshold, i.e., P_0 in Eq. (2). This will have a steeper slope than that in Fig. 8. Unfortunately, as demonstrated above for GaAs, measurements of P_0 are usually hampered by sluggish transition kinetics, formation of metastable phases, and dependence on specimen history and/or nonhydrostatic conditions. However, it is important that accurate experiments be undertaken (e.g., see Ref. 13 for very recent work) since present calculations, which obtain only P_0 , cannot be properly compared to the measured P' in cases of large hysteresis.²² Alternatively, it would be interesting to extend microscopic theories by including the interface energy of a β nucleus within an α matrix along lines similar to those applied in the fourfold-sixfold calculation of Ref. 24, or in recent work on fourfold-fourfold heterointerfaces.⁵² Besides allowing a more direct comparison with the observed P' , this should give considerable insight into the little understood kinetics of the α - β phase change in semiconductors.

V. SUMMARY

The Raman spectra of bulklike AlAs and GaAs epitaxial films have been studied under increasing and decreasing hydrostatic pressure through their $\alpha \leftrightarrow \beta$ phase transitions. The pressure shifts of the ZB-phase LO(Γ) and TO(Γ) peaks of both materials and the TA overtone band of GaAs are measured with high precision. Our $\gamma_{\text{TA}(X)} = -1.2 \pm 0.1$ for GaAs, though considerably different from prior results, conforms more closely to observed material trends for correlation with the α - β transition pressures. A careful search was unable to detect the

ZB AlAs 2TA band at any pressure. Previous results for AlAs have been reported only for thin multilayers^{39,41} (see Table II).

The increasing pressure α - β thresholds of AlAs and GaAs are $P_a^t = 12.4 \pm 0.4$ GPa and $P_g^t = 17.3 \pm 0.4$ GPa, respectively. Transformation proceeds via a nucleation mechanism in both materials, with the growth kinetics appreciably more sluggish in GaAs than in AlAs. The forward α - β transitions in GaAs and AlAs are reversible on decompression, as long as $P_{\max} < 20$ GPa; transparency and the ZB Raman peaks reappear concurrently, but take several hours to reach maximum strength. The reverse thresholds R^t exhibit approximately 6 GPa and 8 GPa hysteresis in AlAs and GaAs, respectively.

After reversal, the returning LO(Γ) and TO(Γ) peaks are asymmetrically broadened and shifted to lower energy, much as in studies of moderate-dosage ion bombardment in GaAs. Applying a spatial-correlation model,⁴² we conclude that the postreversal phases are strongly microcrystalline—the average size of correlated ZB domains being ~ 65 Å in GaAs and ~ 175 Å in AlAs. Hence the ZB-microcrystallite size obtained in GaAs after decompression from $P_g^t < P_{\max} < 20$ GPa is close to the minimum size observed in ion-implantation studies^{42,43} before complete amorphization. This is not surprising considering the $\sim 18\%$ volume decrease and the fourfold to sixfold coordination change during these transitions.

The Raman results on GaAs show that reducing pressure to 1 bar from $P_{\max} > 20$ GPa produces a metastable non-ZB crystal structure, distinct from the amorphous form.¹⁵ (Amorphization seems to occur after decompression from megabar pressures.^{13,16}) For AlAs we cannot determine whether decompression from above 20 GPa produces reversal to the ZB phase, or a metastable state analogous to that found in GaAs.

The positive surface energy $\sigma_0^{\beta\alpha}$ required to nucleate a β -phase nucleus within an α matrix gives rise to a minimum radius r^* which must be exceeded for sustained growth of β nuclei. Straightforward thermodynamics allows us to deduce $\sigma_0^{\beta\alpha}$ from our estimates of microcrystallite size and the measured hysteresis. We find that $\sigma_0^{\beta\alpha}$ should be ~ 0.05 – 0.08 eV/Å² in GaAs, and ~ 0.04 – 0.15 eV/Å² in AlAs.

The surface of a β nucleus represents an expanding boundary between sixfold and fourfold coordinated polymorphs of the same material. Given the chemical similarity of AlAs and GaAs, we propose that this kinetic boundary resembles, both in structure and in energy, the static β -AlAs/ α -GaAs heterointerface discussed for SL phase transitions in Paper II. Hence, at least in the early stages of nucleus growth, a candidate for the expanding β/α *homointerface* is the NiAs(sixfold)/ZB(fourfold) arrangement considered for (111) AlAs/GaAs SL's in Ref. 24. The order-of-magnitude agreement between the theoretical energy density found in that work, and our present estimates of $\sigma_0^{\beta\alpha}$, supports this connection. An alternative grain-boundary picture for a β nucleus within an α matrix yields reasonable numbers for the spacing of dislocations at the nucleus surface; in its SL analog, we will consider the role of heterointerface misfit dislocations.

ACKNOWLEDGMENTS

This work was supported in part by ONR Contract No. N00014-89-J-1797, and by grants from the Xerox Webster Research Center, and the Center for Electronic and Electro-optic Materials at SUNY-Buffalo. The authors are grateful to R. Zallen and M. Holtz for helpful discussions.

*Present address: Department of Physics, Oakland University, Rochester, MI 48309.

† Present address: Department of Physics, Harvard University, Cambridge, MA 02138.

¹A. Jayaraman, R. C. Newton, and G. C. Kennedy, *Nature* (London) **191**, 1288 (1961); A. Jayaraman, W. Klement, and G. C. Kennedy, *Phys. Rev.* **130**, 540 (1963).

²S. Minomura and H. G. Drickamer, *J. Phys. Chem. Solids* **23**, 451 (1962); G. A. Samara and H. G. Drickamer, *ibid.* **23**, 457 (1962).

³J. C. Jamieson, *Science* **139**, 762 (1963); **139**, 845 (1963).

⁴J. C. Phillips, *Phys. Rev. Lett.* **27**, 1197 (1971); for a general discussion see J. C. Phillips, *Bonds and Bands in Semiconductors*, edited by A. M. Alper, J. L. Margrave, and A. S. Nowick (Academic, New York, 1973).

⁵J. A. Van Vechten, *Phys. Rev. B* **7**, 1479 (1973).

⁶R. E. Hanneman, M. D. Banus, and H. C. Gatos, *J. Phys. Chem. Solids* **25**, 293 (1964).

⁷H. G. Drickamer, in *Solid State Physics: Advances in Research and Applications*, edited by F. Seitz and D. Turnbull (Academic, New York, 1965), Vol. 17, p. 1.

⁸W. Klement and A. Jayaraman, in *Progress in Solid State Chemistry*, edited by H. Reiss (Pergamon, London, 1967),

Vol. 3, p. 289; A. Jayaraman, in *Synthesis and Properties of Metastable Phases*, edited by E. S. Machlin and T. J. Rowland (The Metallurgical Society of AIME, Pittsburgh, 1980), p. 75.

⁹S. C. Yu, I. L. Spain, and E. F. Skelton, *Solid State Commun.* **25**, 49 (1978); S. C. Yu, C. Y. Liu, I. L. Spain, and E. F. Skelton, in *High Pressure Science and Technology*, edited by K. D. Timmerhaus and M. S. Barber (Plenum, New York, 1979), Vol. 1, p. 274.

¹⁰S. Geller, D. E. McWhan, and G. W. Hull, *Science* **140**, 62 (1963); K. J. Chang, M. M. Dacorogna, M. L. Cohen, J. M. Mignot, G. Chouteau, and G. Martinez, *Phys. Rev. Lett.* **54**, 2375 (1985).

¹¹S. B. Zhang, P. Y. Yu, D. Erskine, and M. L. Cohen, *Solid State Commun.* **71**, 369 (1989).

¹²M. Baublitz, Jr. and A. L. Ruoff, *J. Appl. Phys.* **53**, 6179 (1982); S. T. Weir, Y. K. Vohra, C. A. Vanderborgh, and A. L. Ruoff, *Phys. Rev. B* **39**, 1280 (1989).

¹³J. M. Besson, J. P. Itie, A. Polian, G. Weill, J. L. Mansot, and J. Gonzalez, *Phys. Rev. B* **44**, 4214 (1991); this very recent study of the α - β transition in bulk GaAs uses several experimental techniques to delineate the range of the equilibrium threshold P_0 . It is concluded that $P_0 = 12 \pm 1.5$ GPa, in substantial agreement with $(P^t + R^t)/2$ from the present work

- (see Sec. IV A and Table I). These authors also find Raman evidence for disorder after reversal, but detect no persistent metastable phase in samples retrieved at 1 bar following full transformation.
- ¹⁴J. S. Kasper and S. M. Richards, *Acta Crystallogr.* **17**, 752 (1964); the β -Sn phases of InSb and GaSb are metastably retained when pressure is released at 77 K but not at room temperature. See A. Jayaraman (1980) in Ref. 8.
- ¹⁵U. D. Venkateswaran, L. J. Cui, B. A. Weinstein, and F. A. Chambers, *Phys. Rev. B* **43**, 1875 (1991).
- ¹⁶Y. K. Vohra, H. Xia, and A. L. Ruoff, *Appl. Phys. Lett.* **57**, 2666 (1990); these authors find by energy-dispersive x-ray diffraction that decompression from megabar pressures ($P_{\max} \approx 115$ GPa) can produce amorphous GaAs.
- ¹⁷D. Turnbull, in *Solid State Physics: Advances in Research and Applications*, edited by F. Seitz and D. Turnbull (Academic, New York, 1957), Vol. 3, p. 1.
- ¹⁸M. J. P. Musgrave, *Proc. R. Soc. London Ser. A* **272**, 503 (1963).
- ¹⁹P. Hohenberg and W. Kohn, *Phys. Rev.* **136**, 864 (1965); W. Kohn and L. J. Sham, *ibid.* **140**, 1133 (1965); J. Ihm, A. Zunger, and M. L. Cohen, *J. Phys. C* **12**, 4409 (1979); K. Kunc and R. M. Martin, in *Ab initio Calculation of Phonon Spectra*, edited by J. T. Devreese, V. E. Van Doren, and P. E. Van Camp (Plenum, New York, 1983), pp. 65–99.
- ²⁰M. T. Yin and M. L. Cohen, *Phys. Rev. Lett.* **50**, 1172 (1983); **50**, 2006 (1983).
- ²¹R. Biswas, R. M. Martin, R. J. Needs, and O. H. Nielsen, *Phys. Rev. B* **30**, 3210 (1984); **35**, 9559 (1987).
- ²²S. Froyen and M. L. Cohen, *Phys. Rev. B* **28**, 3258 (1983).
- ²³B. A. Weinstein, S. K. Hark, R. D. Burnham, and R. M. Martin, *Phys. Rev. Lett.* **58**, 781 (1987); B. A. Weinstein, S. K. Hark, and R. D. Burnham, in *The Physics of Semiconductors*, edited by O. Engström (World Scientific, Singapore, 1987), Vol. 1, p. 707.
- ²⁴R. M. Martin, in *The Physics of Semiconductors*, edited by O. Engström (World Scientific, Singapore, 1987), Vol. 1, p. 639.
- ²⁵P. M. Raccach, J. W. Garland, Z. Zhang, F. A. Chambers, and D. J. Vezzetti, *Phys. Rev. B* **36**, 4271 (1987); I. K. Schuller, M. Grimsditch, F. Chambers, G. Devane, H. Vanderstraeten, D. Neerincx, J.-P. Locquet, and Y. Bruynseraede, *Phys. Rev. Lett.* **65**, 1235 (1990).
- ²⁶A. R. Goñi, K. Strössner, K. Syassen, and M. Cardona, *Phys. Rev. B* **36**, 1581 (1987). Our 15- μ m-thick specimens become transparent above 4.5 GPa for $\lambda_l = 647.1$ nm and above 10.5 GPa for $\lambda_l = 488$ nm.
- ²⁷G. J. Piermarini and S. Block, *Rev. Sci. Instrum.* **46**, 973 (1975); G. J. Piermarini, S. Block, J. D. Barnett, and R. A. Forman, *J. Appl. Phys.* **46**, 2774 (1975).
- ²⁸For this step we use undiluted commercial Clorox brand bleach.
- ²⁹U. D. Venkateswaran, D. J. Thiel, K. E. Brister, B. A. Weinstein, and D. H. Bilderback (unpublished).
- ³⁰L. J. Cui and B. A. Weinstein (unpublished).
- ³¹B. A. Weinstein and M. Cardona, *Phys. Rev. B* **7**, 2545 (1973).
- ³²L. J. Cui, U. D. Venkateswaran, B. A. Weinstein, and F. A. Chambers, *Semicond. Sci. Technol.* **6**, 469 (1991).
- ³³M. Cardona, in *Light Scattering in Solids II*, edited by M. Cardona and G. Güntherodt, *Topics in Applied Physics Vol. 50* (Springer, Berlin, 1983), Chap. 2.
- ³⁴R. Trommer, E. Anastassakis, and M. Cardona, in *Light Scattering in Solids*, edited by M. Balkanski, R. C. C. Leite, and S. P. S. Porto (Flammarion, Paris, 1976); R. Trommer, H. Müller, and M. Cardona, *Phys. Rev. B* **21**, 4869 (1980); P. Y. Yu and B. Welber, *Solid State Commun.* **25**, 209 (1978).
- ³⁵M. Cardona (private communication).
- ³⁶Actually, for the relevant cubic geometry only optic modes polarized perpendicular to the (001) plane can contribute to the first-order Γ_{15} -symmetry Raman tensor. These modes will be transverse for forward scattering and longitudinal for backscattering because the momentum transfer will be parallel and perpendicular to the (001) plane in the two respective cases.
- ³⁷See B. A. Weinstein and R. Zallen, in *Light Scattering in Solids IV*, edited by M. Cardona and G. Güntherodt, *Topics in Applied Physics Vol. 54* (Springer, Heidelberg, 1984), Chap. 8.
- ³⁸S. Adachi, *J. Appl. Phys.* **58**, R1 (1985).
- ³⁹M. Holtz, U. D. Venkateswaran, K. Syassen, and K. Ploog, *Phys. Rev. B* **39**, 8458 (1989).
- ⁴⁰P. Wickboldt, E. Anastassakis, R. Sauer, and M. Cardona, *Phys. Rev. B* **35**, 1362 (1987); M. Hünemann, W. Richter, J. Saalmüller, and E. Anastassakis, *ibid.* **34**, 5381 (1986).
- ⁴¹P. Seguy, J. C. Maan, G. Martinez, and K. Ploog, *Phys. Rev. B* **40**, 8452 (1989).
- ⁴²K. K. Tiong, P. M. Amirtharaj, F. A. Pollak, and D. E. Aspnes, *Appl. Phys. Lett.* **44**, 122 (1984).
- ⁴³M. Holtz, R. Zallen, O. Brafman, and S. Matteson, *Phys. Rev. B* **37**, 4609 (1988); R. Zallen, M. Holtz, A. E. Geissberger, R. A. Sadler, W. Paul, and M.-L. Théye, *J. Noncrystalline Solids* **114**, 795 (1989).
- ⁴⁴H. Richter, Z. P. Wang, and L. Ley, *Solid State Commun.* **39**, 625 (1981).
- ⁴⁵R. Biswas, R. M. Martin, R. J. Needs, and O. H. Nielsen, *Phys. Rev. B* **35**, 9559 (1987).
- ⁴⁶C. G. Van de Walle and R. M. Martin, *Phys. Rev. B* **34**, 5621 (1986).
- ⁴⁷W. A. Harrison, *Electronic Structure and the Properties of Solids* (Freeman, San Francisco, 1980), p. 176.
- ⁴⁸Martin's hybrid structure contains two atom pairs and two interfaces per unit hexagonal cell of cross section $\sqrt{3}a_0^2/4$ normal to (111). For a_0 we use the GaAs ambient value of 5.653 Å.
- ⁴⁹F. R. N. Nabarro, *Theory of Crystal Dislocations* (Dover, New York, 1967), p. 31.
- ⁵⁰W. T. Read and W. Shockley, *Phys. Rev.* **78**, 275 (1950).
- ⁵¹B. A. Weinstein, in *High Pressure Science and Technology*, edited by K. D. Timmerhaus and M. S. Barber (Plenum, New York, 1979), Vol. 1, p. 141.
- ⁵²A. A. Mbaye, D. M. Wood, and A. Zunger, *Phys. Rev. B* **37**, 3008 (1988); S.-H. Wei and A. Zunger, *Phys. Rev. Lett.* **61**, 1505 (1988).